LINEAR FOCAL CHERENKOV-RING CAMERA FOR SINGLE SHOT OBSERVATION OF LONGITUDINAL PHASE SPACE DISTRIBUTION FOR NON-RELATIVISTIC ELECTRON BEAM *

K. Nanbu#, K. Kashiwagi, H. Hinode, Y. Shibasaki, T. Muto, I. Nagasawa, S. Nagasawa,
K. Takahashi, C. Tokoku, A. Lueangaramwong, H. Hama,
Electron Light Science Centre, Tohoku University, Sendai, Japan

Abstract

Test accelerator as a coherent Terahertz (THz) source (t-ACTS) has been constructed at Tohoku University, in which generation of intense coherent THz radiation from sub-picosecond electron bunches will be demonstrated. Since final electron bunch length of accelerated beam is mostly dictated by the longitudinal phase space distribution at the exit of electron-gun, Measurement of initial electron distribution in the longitudinal phase space is indispensable for stable production of very short electron bunches. A novel method for measurement of electron kinetic energy applying a velocity dependence of the opening angle of Cherenkov light from a radiator medium has been proposed for relatively lower energy electrons. Combined use of a streak camera and a "turtle-back" mirror designed specifically that confines the Cherenkov light onto a linear focal line may allow us to observe the longitudinal phase space distribution directly. In this report, we describe the concept and designing of the linear focal Cherenkov-ring (LFC) camera system, as well as the current status of the system development.

t-ACTS PROJECT

In the t-ACTS project, the intense coherent THz radiation will be generated from an undulator and an isochronous accumulator ring via producing sub-picosecond bunches [1, 2, 3]. The t-ACTS consists of a thermionic cathode rf gun, an alpha magnet and a 3-meter-long accelerating structure, and velocity bunching scheme in the accelerating structure is being used for generate the sub-picosecond electron bunches. The thermionic rf gun composed of two independent cavities is capable of manipulating the beam longitudinal phase space, named an Independently-Tunable Cells (ITC) RF gun [4]. Employing a scheme of velocity bunching in the travelling-wave accelerating structure, the bunch compression will be performed [5]. The longitudinal phase space distribution at the exit of the rf-gun governs the final bunch length of electron beam after the bunch compression process, so that production of proper initial electron distribution in the longitudinal phase space is crucial to achieve very short electron bunch length of hundreds femtosecond.

*Work supported by JSPS KAKENHI Grant Numbers 24651096, 25790078.
#nanbu@lns.tohoku.ac.jp

LINEAR FOCAL CHERENKOV-RING CAMERA

Concept and Principle

In order to confirm directly whether the proper longitudinal phase space of the beam created by the ITC-RF gun for bunch compression, the LFC camera has been developed [6, 7].

The Cherenkov light is widely used for beam diagnostics and particle counters in high energy physics experiments. It is well known that the Cherenkov angle θ_c is inversely proportional to the particle velocity β (= v/c) as

$$\cos\theta_c = \frac{1}{n(\omega)\beta}, \qquad (1)$$

where n(ω) is the refractive index of the Cherenkov radiator medium at a radiation frequency. Since the Cherenkov angle contains information of the charged particle velocity, the photons having the same Cherenkov angle has to be focused onto an identical focal position of a detector in order to identify the particle momentum. If the focal points of different Cherenkov angles can be placed on a straight line, the momentum distribution of the beam will be observed at once. Furthermore, if information on relative arrival times onto the Cherenkov

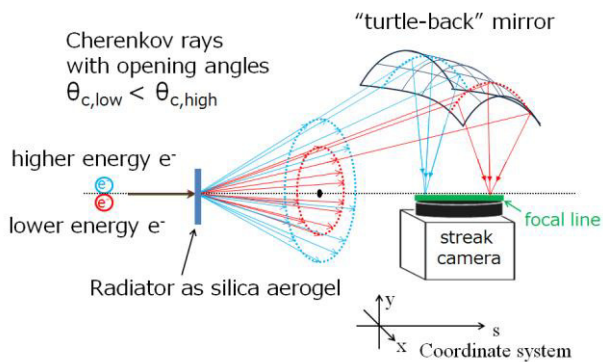

Figure 1: Conceptual drawing of the LFC camera. Electron emits the Cherenkov light when through the radiator made by silica aerogel. The turtle-back mirror is used to resolve the Cherenkov rays with the different opening angles with specific focal positions along a focal line. The streak camera can detect the relative arrival time of the rays with sub-picosecond time resolution.

ISBN 978-3-95450-141-0

radiator for each particle is preserved, we are able to perform direct observation of the longitudinal phase space distribution by using a high-resolution streak camera.

Figure 1 shows schematic principle of the LFC-camera. The LFC- camera is composed of a Cherenkov radiator, turtle-back mirror, and optical devices such as a streak camera. The turtle-back mirror gathers photons emitted some part of azimuthal angle in the Cherenkov ring and confines onto the longitudinal axis. Surface of the turtle-back mirror is parabolic in the s-axis and spherical in the x-axis (shape of mirror looks like a turtle's carapace, so named the turtle-back mirror).

Design and Manufacturing the Turtle-back Mirror

The reflecting surface of the turtle-back mirror is expressed by a following formula

$$x^2 + y^2 - \left(-\frac{1}{2A} s^2 + \frac{A}{2} \right)^2 = 0 \quad \left(A \equiv \sqrt{y_0^2 + s_0^2} + y_0 \right). \quad (2)$$

The origin of the coordinate is the center of the radiator medium. The parabolic curve can resolve Cherenkov ray with the different Cherenkov angles. Role of the spherical curve is to confine the Cherenkov light on the s-axis, in other words focus it in the x-direction. The parameter A of the turtle-back mirror is crucially important for the energy resolution at the LFC camera [8], meanwhile the parameter A makes little impact on the time resolution. The parameter A is a magnification factor of the energy resolution, nothing but that the energy resolution can be optimized when optimum and larger A is selected. On the other hand, the small A leads an advantage in fabrication, Physical size of the turtle-back mirror limits the tolerance of machining error.

Momentum and time resolutions of the LFC camera for measuring longitudinal phase space at the exit of the rf-gun are required to be less than 1 keV/c and 1 ps, respectively. As a result, the parameter A of 350 mm was chosen, in which the momentum in a range from 2.294 to 2.412 MeV/c can be observed with sufficient resolution by the streak camera having a photon entrance slit of 3 mm width.

A prototype turtle-back mirror was fabricated for proof-of principle experiment. Since distortion caused during machining on the fabricated mirror surface may critically affect the resolution, an aluminium block cut to the eight pieces and assembled together with a special jig was lathed along its central axes to shape the parabolic curve. The mirror surface was polished and coated by vacuum aluminium evaporation

Performance Test of the Turtle-back Mirror

To evaluate the momentum and time resolutions caused by the surface roughness of the turtle-back mirror, roughness parameters such as the amplitude of the roughness and the correlation length are required. We measured the surface profile of the turtle-back mirror using a contact type surface profilometer (Talysurf PGI 1250A).

The surface of a high quality commercial plain mirror was also measured to compare with the turtle-back mirror. Figure 2 shows measurement results of surface profilometer. The roughness of the turtle-back mirror was deduced by Fourier transform. Roughness analysis result indicates a root-mean-square amplitude of the roughness per correlation length is 0.00032. Using a ray trace calculation it was found out that the momentum resolution is degraded from 1.05 keV/c to 7 keV/c. On the other hand, the commercial plane mirror roughness was measured to be as low as 0.000016. Consequently, it is concluded the surface of the turtle-back mirror is not well manufactured and must be improved for sufficient momentum and time resolution.

In order to confirm the parameter A of the turtle-back mirror, we have measured the parameter A as follows.

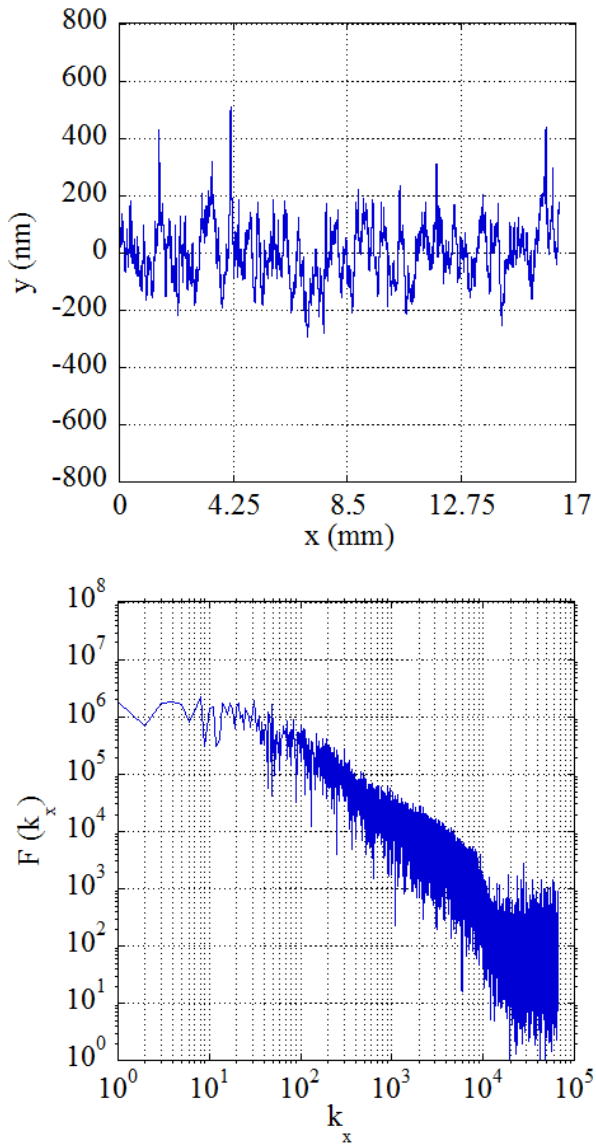

Figure 2: (upper) one-dimensional surface profile of the turtle-back mirror along the x-direction (lower) Fourier spectrum of the surface profile.

ISBN 978-3-95450-141-0

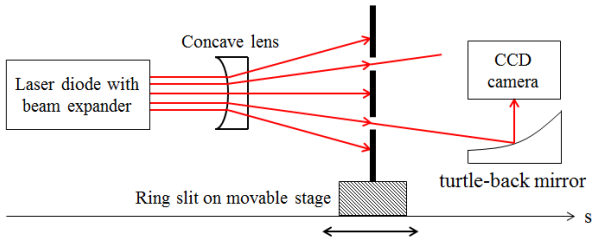

Figure 3: Schematic view of the parameter A measurement. The opening angle of laser is varied by moving the ring slit position along the s-axis.

We have used a ring-like diverging laser light instead of the Cherenkov light as shown in Fig. 3. It makes possible to generate the particular opening angle (represented by the Cherenkov angle θ_c) by changing the position of the ring slit on the translation stage. The CCD camera is placed on the focal line above the turtle-back mirror to acquire the focal position and the focal profile for respective opening angles. Measurement were performed for a wide range of the opening angle, and the derived parameter A was 349.50±0.13 mm, while target value is 350 mm. Although the roughness of the prototype mirror surface is quite insufficient, overall shape of the mirror is well manufactured. Surface polishing by a precision machinery technique will be performed.

CHERENKOV RADIATOR

Silica Aerogel

The LFC-camera employs the Cherenkov radiator placed in vacuum to avoid the electron scattering in vacuum windows. The radiator medium is required to have high transparency as well as low refractive index around 1.05, so that we have chosen the hydrophobic silica aerogel with extremely low density [10].

Accuracy of Electron Momentum

Since the LFC camera employs the silica aerogel in vacuum as Cherenkov radiator, if the refractive index of silica aerogel in vacuum is different from an atmospheric one, there should be some ambiguity in measured electron momentum. It was reported that refractive index of aerogel in vacuum is changed by approximately 2% compared with atmospheric one [9].

The focal position of the turtle-back mirror is expressed as

$$s_f(\beta) = A \cdot n \cdot \beta \left[1 - \sqrt{1 - \left(\frac{1}{n \cdot \beta} \right)} \right], \qquad (3)$$

where $s_f(\beta)$ is the position of the focal line along the s-axis for the Cherenkov photon emitted from the electron with a velocity β and n is the refractive index of the Cherenkov radiator. The turtle-back mirror converts the Cherenkov angle to the focal position of the focal line. Figure 4 shows a plot of $s_f(\beta)$ and its derivative as a function of the electron momentum p. If refractive index

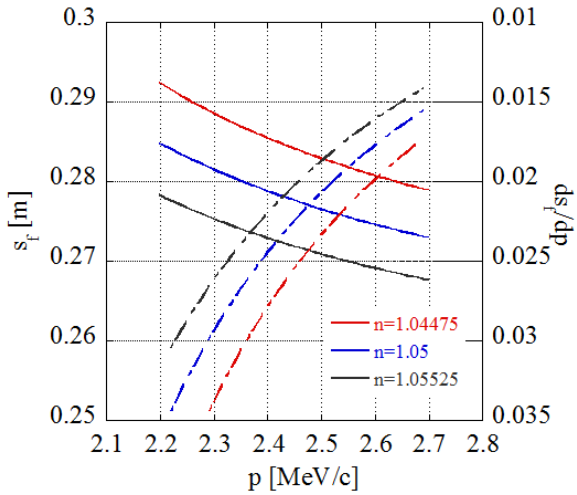

Figure 4: Solid lines denote the variation of focal positions for different refractive indices of the radiator medium calculated using Eq. (3). Dotted lines indicate those derivatives of the focal position with respect to the momentum p.

of the radiator in vacuum differs by as low as 0.5% compared with the one at atmospheric pressure, the position on the focal line is shifted about 10 mm, which is equivalent to a change of the momentum of 250 keV/c. Absolute value of the in-vacuum refractive index of silica aerogel is crucial to calibrate the electron momentum observed by the LFC-camera.

Refractive Index Measurement

Number of method for measurement of the refractive index, such as a minimum deviation angle method, a critical angle method and a v-block method, have been developed for many years. However, these methods are not much suitable for measurement of the thin silica aerogel. Therefore, we performed measurement of the thin silica aerogel refractive index by detecting an optical path difference using a Mach-Zehnder interferometer [11]. The optical path difference Δd at the rotation angle θ is expressed as

$$\Delta d = t\left(n\cos\theta_r - \theta_i\right) - t \cdot \left(n - 1\right), \qquad (4)$$

where θ_i is an incident angle, θ_r is a reflecting angle. The refractive index n at the optical path difference Δd can be derived as

$$n = -\frac{(m\lambda)^2 + 2t(m\lambda - t)(\cos\theta_i - 1)}{2t\left\{t(\cos\theta_i - 1) + m\lambda\right\}}, \qquad (5)$$

where λ is a wavelength of laser, m is an order of interference. Figure 5 shows the schematic of interferometer for refractive index measurement. Rotating angle of the silica aerogel is being controlled by a stepper motor (1 step = 0.001125deg). The silica aerogel is installed on the rotary manipulator via a special holder in the vacuum chamber.

ISBN 978-3-95450-141-0

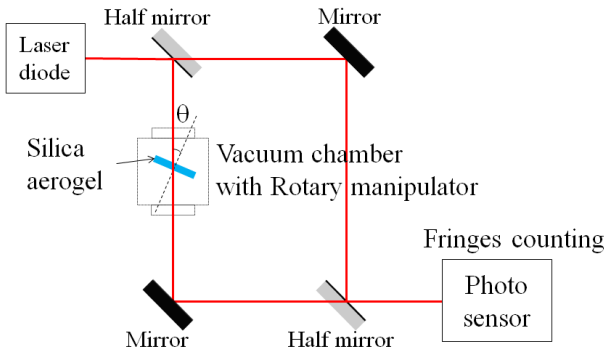

Figure 5: The interferometer for refractive index measurement. A silica aerogel is placed in the vacuum chamber with a rotary manipulator. It is possible to rotate in vacuum. A light source for interferometer is a diode laser with a laser beam expander and a photodiode with an amplifier is used to detect the laser light interference.

Two silica aerogels, referred in the following as the Sample 1 and Sample 2 one, have been measured. The rotation angle was varied between -45° to +45° in steps of 0.01125°. Measured interfered spectrum was analysed by second-order polynomial curve fitting, and then the optical path difference was derived. The refractive index of samples was calculated using Eq. (5) applied for a 10^{th} order interfered spectrum. The average value of refractive index deduced from 6 times measurements carried out for each sample was listed in Table 1.

Table 1: Measurement Result

	Atmospheric pressure	**Vacuum (3×10^{-5}Pa)**	**Difference value**
Sample 1	1.0448(13)	1.0440(20)	0.0008(23)
Sample 2	1.0488(6)	1.0450(6)	0.0038(8)

It was found out the measured value for the sample 2 at the atmospheric pressure is in good agreement with a refractive index of 1.049 that was already derived using a mass density. This suggests the measurement system has sufficient performance for lower refractive index case such as n ~ 1.05.

We have not observed significant difference for the refractive index in vacuum from one at the atmospheric pressure for the sample 1. Though the refractive index in vacuum of the sample 2 obviously diminished from the one at the atmospheric pressure, the difference of 0.4 % is pretty small. This experimental result indicates a structural change of the silica aerogel due to the vacuum pressure is unlikely because the aerogel was manufactured by a water-free hydrophobic treatment [12].

CONCLUSION

A novel beam diagnostic system for direct measurement of longitudinal phase space distribution (the LFC-camera) has been studied and developed. Characteristics of the prototype turtle-back mirror was investigated. The large surface roughness of the turtle-back mirror degrades the momentum resolution to up to 7 keV, while the predicted it is 1 keV resulted from perfect system condition. The measured parameter A was indicated 349.50±0.13 mm, which is in good agreement with a designed value of 350 mm. According to the measurement with Mach-Zehnder interferometer, the refractive index of aerogel in vacuum diminishes by 0.36% from one in the atmospheric pressure, which may shift the absolute momentum by 200 keV/c. However, we have confirmed the refractive index of the silica aerogel can be known beforehand, so that calibration of the electron momentum observed by LFC-camera is possible with sufficient accuracy.

ACKNOWLEDGEMENT

The authors thank the Industrial Technology Institute of Miyagi Prefectural Government for the mirror surface measurement. We appreciate Dr. M. Tabata of Chiba University for providing the silica aerogel samples.

REFERENCES

[1] H. Hama et al., N. J. of Phys. 8 (2006), 292.
[2] H. Hama and M. Yasuda, Proc. of FEL2009, (2009), 394.
[3] F. Hinode et al., Nucl Instr. and Meth., A 637 (2011), S72.
[4] T. Tanaka et al., Proc. 27th Int. FEL Conf., Stanford (2005), 371.
[5] F. Miyahara et al., Proc. of IPAC'10, (2010), 4509.
[6] H. Hama et al, Proc of BIW10, (2010), TUCNB03.
[7] K. Nanbu et al., Proc. of FEL2011, (2011), 576.
[8] A. Lueangaramwong, "Development of Linear Focal Cherenkov-ring Camera for Direct Observation of Longitudinal Phase Space of Non-relativistic Electron Beam", Master's thesis, Tohoku University, 2014.
[9] D. Richter et al., Nucl Instr. and Meth., A 513 (2003), 635.
[10] A. Lueangaramwong, et al., Proc, of PASJ10, (2013), 194.
[11] Laser Handbook second edition, The Laser Society of Japan, (2005), 72.
[12] M. Tabata, et al. Nucl Instr. and Meth., A 623 (2010), 339.

ISBN 978-3-95450-141-0